ACS APPLIED MATERIALS & INTERFACES

Research Article

www.acsami.org

Novel Pb^{2+} Ion Imprinted Polymers Based on Ionic Interaction via Synergy of Dual Functional Monomers for Selective Solid-Phase Extraction of Pb^{2+} in Water Samples

Xiaoqiang Cai,[†,‡] Jinhua Li,[*,†] Zhong Zhang,[†,§] Fangfang Yang,[†,‡] Ruichen Dong,[†] and Lingxin Chen[*,†,‡]

[†]Key Laboratory of Coastal Environmental Processes and Ecological Remediation, Shandong Provincial Key Laboratory of Coastal Environmental Processes, Yantai Institute of Coastal Zone Research, Chinese Academy of Sciences, Yantai 264003, China

[‡]College of Chemistry and Chemical Engineering, Qufu Normal University, Qufu 273165, China

[§]University of Chinese Academy of Sciences, Beijing 100049, China

Supporting Information

ABSTRACT: A novel kind of Pb^{2+} ion imprinted polymers (IIPs) was prepared based on ionic interactions via the synergy of dual functional monomers of methacrylic acid and vinyl pyridine for selective solid-phase extraction (SPE) of Pb^{2+} in water samples. Suspension polymerization was employed for the formation of template Pb^{2+}/monomer complex by self-assembly in the presence of ethylene glycol dimethacrylate cross-linker. The resulted Pb^{2+} IIPs showed fast kinetics, high binding capacity, and the adsorption processes obeyed intraparticle diffusion kinetics and Langmuir isotherm models. The IIPs displayed excellent selectivity toward Pb^{2+} over other metal ions such as Cu^{2+}, Cd^{2+}, Zn^{2+}, and Mn^{2+} with selective coefficients above 30, as well as high anti-interference ability for Pb^{2+} confronting with common coexisting various ions. Through 10 adsorption−desorption cycles, the reusable IIPs exhibited a good recoverability with the standard error within 5%. These features suggested the IIPs were ideal candidates for extraction and removal of Pb^{2+} ions. Consequently, the IIPs were utilized as SPE sorbents and related parameters were optimized. An excellent linearity was presented in the range of 0.2−50 $\mu g\ L^{-1}$ (R^2 = 0.9998), as well as the limits of detection and quantification were achieved of 0.06 and 0.19 $\mu g\ L^{-1}$, respectively. A good repeatability was obtained with the relative standard deviation of 2.8%. Furthermore, real water samples were successfully analyzed and satisfactory recoveries varying from 95.5 to 104.6% were attained. The IIPs-SPE demonstrated potential application perspectives for rapid and high-effective cleanup and enrichment of trace Pb^{2+} ions in complicated matrices.

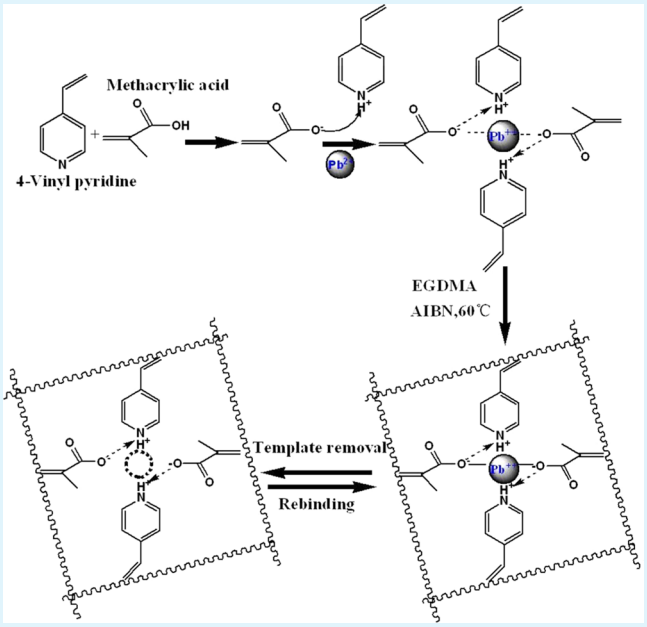

KEYWORDS: *Pb^{2+}, ion imprinted polymers, dual functional monomers, ionic interaction, synergy, suspension polymerization*

INTRODUCTION

The monitoring and remediation of heavy metal pollution is increasingly becoming a crucial global issue since heavy metals can cause many biological abnormalities and tend to accumulate in food chains.[1−4] Among heavy metals, lead (Pb), with important environmental and toxicological significances, has become a research hotspot and received wide concerns.[5−7] Various kinds of methods are available for the determination and/or removal of Pb^{2+} in water samples.[5−11] For example, Pan et al. have fabricated a nanomaterial-ionophore based electrode for anodic stripping voltammetric detection of Pb^{2+}.[9] Fu et al. have developed a fluorescence sensing strategy for Pb^{2+} based on accelerated leaching of gold nanoparticles on graphene surface.[10] Rehman et al. have utilized chemically modified biosorbents for sorption removal of Pb^{2+} from water.[11] So the development of selective separation and detection methods for trace amounts of lead ions has attracted widespread attention.[8,12,13] However, the presence of complex matrices in environmental samples is generally a huge obstruction to performing direct analysis of Pb^{2+}.[14] Although a number of ways such as membrane, chemical precipitation, and ion exchange to remove heavy metal ions are industrially suitable for nonpreferential separation, the poor selective separation is still a large defect.[15,16] Therefore, it is urgently

Received: September 27, 2013
Accepted: December 17, 2013
Published: December 17, 2013

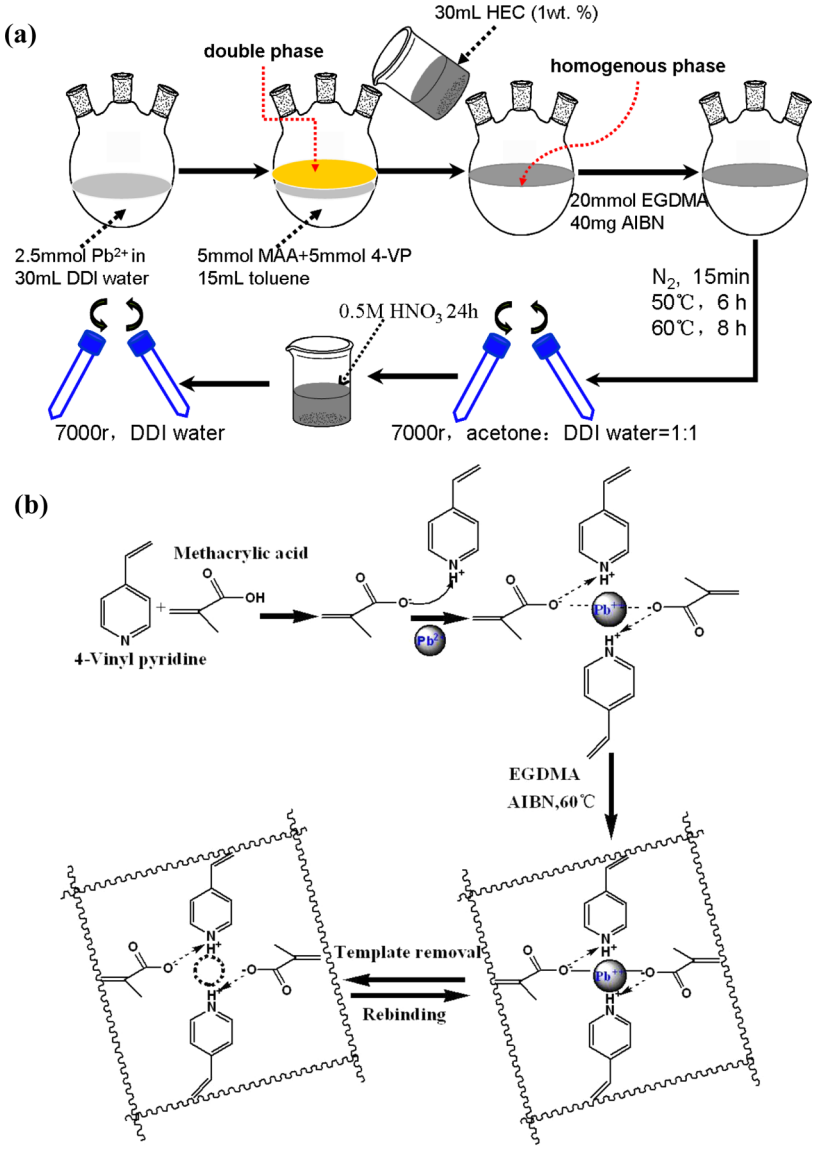

Figure 1. Schematic illustrations of experimental procedure for Pb^{2+} IIPs preparation (a) and imprinting process of the IIPs for Pb^{2+} (b).

required to develop highly selective separation/removal materials and methods for Pb^{2+}.

Meanwhile, as we all know, molecular imprinting is a commonly used technology to build a molecular recognition mechanism in triaxial cross-linked polymers named molecularly imprinted polymers (MIPs).[17,18] More recently, MIPs have been identified as ideal materials and are widely used in contaminant removal and trace analysis, since they are suitable for applications where analyte selectivity is essential.[17−22] Ion imprinted polymers (IIPs), an important branch of MIPs, are similar to MIPs, but they recognize inorganic ions after imprinting, especially metal ions.[18,23−25] A number of IIPs for metal ions have been prepared and applied to determination and removal,[15,18,23−32] such as Pb^{2+} IIPs.[28−32] However, the widely and generally used functional monomers such as methacrylic acid (MAA) and vinyl pyridine (VP) can offer coordination to many metal ions and thereby result in low selectivity. Moreover, in general, single functional monomers are used for preparing imprinted polymers. Thus, it has become quite imperative to develop new functional monomers and/or utilize dual/multiple functional monomers for improving the selective recognition capabilities and adsorption capacities of IIPs. For instances, our group has devised and synthesized a functional monomer T-IPTS, 3-isocyanatopropyltriethoxysilane (IPTS) bearing thymine (T) bases, for specially imprinting Hg^{2+}, and the resultant Hg-IIPs based on $T-Hg^{2+}-T$ interaction have highly effectively preconcentrated trace Hg^{2+} from water samples.[27] Behbahani et al. have prepared Pb^{2+}-imprinted polymeric particles as a sorbent for selective extraction and preconcentration of ultratrace amounts of Pb^{2+} ions from vegetable, rice, and fish samples.[32] The common 2-VP was used as the functional monomer with the combination of diphenylcarbazone as the ligand in bulk polymerization. Hoai et al. have prepared Cu^{2+}-imprinted porous polymethacrylate microparticles using dual functional monomers of MAA and 4-VP by a suspension method, and attained batch and column separation applications.[15] Zhu et al. have synthesized Pb^{2+} ion-imprinted microbeads using dual functional monomers of 1,12-dodecanediol-*O*,*O*′-diphenyl-phosphonic acid and 4-VP by a W/O/W polymerization method, and obtained a suitable construction with micropores fitting the template and recognition sites.[30]

dx.doi.org/10.1021/am4042405 | *ACS Appl. Mater. Interfaces* 2014, 6, 305−313

Inspired by these studies, we expect to prepare a kind of highly selective IIPs for Pb^{2+} recognition and removal, by virtue of the synergy of MAA and 4-VP. The two types of functional monomers, forming anion and cation, respectively, were employed to achieve the reaction optimization, which easily interacted with the Pb^{2+} template to constitute a monomer/metal complex through ionic interactions via self-assembly. A simple suspension polymerization was adopted, and as a comparison the conventional polymerization method, bulk polymerization, was also used for the preparation of Pb^{2+} polymers in the meantime. The morphologies, structures, and thermostability of IIPs were well characterized by SEM, FT-IR, BET, and TGA. Static and dynamic adsorptions were systematically investigated. The IIPs presented excellent selectivity toward Pb^{2+} over Cu^{2+}, Cd^{2+}, Zn^{2+}, and Mn^{2+}, as well as high anti-interference ability. To further confirm the practical applicability of the IIPs for the selective adsorption of Pb^{2+}, they were utilized as SPE sorbents for preconcentration of Pb^{2+} from water samples, and satisfactory recoveries were attained. The IIPs-SPE provided great potential for high-effective cleanup and enrichment of trace Pb^{2+} in complicated matrices.

EXPERIMENTAL SECTION

Reagents. Lead salt ($Pb(NO_3)_2$), MAA, 4-VP, ethylene glycol dimethacrylate (EGDMA), and hydroxyethyl cellulose (HEC) were purchased from Sigma-Aldrich (Shanghai, China). 2,2′-Azobis-(isobutyronitrile) (AIBN) was obtained from Shanghai Chemical Reagents Co (Shanghai, China) and was recrystallized in methanol before use. Other affiliated reagents and materials were all supplied by Sinopharm Chemical Reagent (Shanghai, China). All reagents were of at least analytical pure grade and were used as received except where specified. Aqueous solutions throughout the work were prepared using freshly double deionized (DDI) water, which was produced by a Milli-Q Ultrapure water system with the water outlet operating at 18.2 MΩ (Millipore, Bedford, MA).

Instrumentation. A Fourier transform infrared (FT-IR) spectrometer (Thermo Nicolet Corporation, USA) was employed to record the infrared spectra of samples using a pressed KBr tablet method. A scanning electron microscope (SEM, Hitachi S-4800, Japan, operating at 20 kV) was used to examine the size and morphology of the IIPs. The thermostability and purity was evaluated by thermogravimetry analysis (TGA) using a ZRY-2P thermal analyzer (Mettler Toledo). The specific surface areas of the polymers were attained via Brunauer−Emmett−Teller (BET) analysis by performing nitrogen adsorption experiments. The measurement was made on AUTOSORB 1 (Quantachrome Instruments, Germany). The polymers were degassed at 300 °C in vacuum prior to adsorption measurements. Atomic absorption spectroscopy (AAS) (Shimadzu, Japan) was used to determine the concentration of Pb^{2+}.

Preparation of Pb-IIPs. A suspension polymerization procedure was adopted for the preparation of Pb-IIPs by referring to the reported method[15] with necessary modifications, as follows. $Pb(NO_3)_2$ (2.5 mmol) was dissolved in 30 mL of DDI water, followed by adding MAA and 4-VP as functional monomers individually at 5 mmol. The resulting solution was mixed with 30 mL of HEC (surfactant, 1 wt %) aqueous solution and toluene (15 mL) with continuous stirring for 3 h. Then, EGDMA (20 mmol) and AIBN (40 mg) were added in the mixing solution. The solution was degassed for 10 min in an ultrasonic bath and then was purged for 15 min with nitrogen, followed by cooling for 15 min in an ice bath. The polymerization reaction was carried out at 50 °C for 6 h in a water bath, and then at 60 °C for 8 h. The resultant polymer particles were filtered first and then washed with acetone/water (1:1, v/v) several times to remove the residual monomers and cross-linker. Then the particles were dried for 24 h to constant weight in vacuum. The product was treated with 0.5 mol/L HNO_3 under vigorous stirring to remove the Pb^{2+} ions. At last, the polymers were washed with DDI water to neutral and were dried in vacuum. For simplicity, the obtained polymers prepared by suspension polymerization were named S-IIPs. The experimental process was schematically illustrated in Figure 1a. For comparison, the non-imprinted polymers (NIPs) were also synthesized at the same manner but without adding $Pb(NO_3)_2$, also named S-NIPs. Meanwhile, the IIPs were prepared at the same manner but using single functional monomer of MAA or 4-VP, respectively, that is, S-IIPs-MAA and S-IIPs-VP for simplicity.

As a comparison, bulk polymerization procedure was also employed for preparing IIPs. MAA (5 mmol) and 4-VP (5 mmol) as the functional monomers, EGDMA (20 mmol) as cross-linker, AIBN (40 mg) as initiator, and DMF/acetone (1:1, v/v) as porogen were used for bulk polymerization. Similarly to suspension polymerization, the reaction was conducted in a water bath at 50 °C for 6 h and then 60 °C for 8 h. The products were ground, and then they were washed in the same way as the synthesis by suspension polymerization. For simplicity, the resultant polymers were named B-IIPs.

Adsorption Experiments. Adsorption of Pb^{2+} from aqueous solutions was carried out in batch experiments. The static adsorption test was performed by allowing a constant amount of IIPs to reach the adsorption equilibrium with Pb^{2+} standard solution of known concentrations. That is, 20 mg Pb-IIPs were dispersed in 5 mL standard solutions containing different amounts of Pb^{2+} in a 10 mL flask at 25 °C. Being continuously shaken for 3 h, the mixture solutions were centrifuged at 6000 r/min. The concentration of the upper solution was measured by AAS, and the binding capacity (Q) of Pb^{2+} was figured up by subtracting the free concentrations from the initial concentrations. The maximum binding capacity (Q_{max}) and dissociation constant (K_d) could be estimated according to the Scatchard equation, expressed as:

$$Q/C_e = Q_{max}/K_d - Q/K_d \quad (1)$$

where Q is the binding capacity (mg/g) of Pb^{2+} on polymers, C_e stands for the equilibrium concentration of Pb^{2+} in the solution, K_d is the dissociation constant, and Q_{max} is the theoretical maximum binding amount of Pb^{2+} on polymers. The same procedure was adopted to examine the adsorption amounts of NIPs. And similar experiments were carried out to investigate the effect of pH on adsorption capacity, in the Pb^{2+} solutions with pH values ranging from 2 to 7.

In a meanwhile, the dynamic adsorption test for Pb^{2+} was carried out by monitoring the temporal binding amount of Pb^{2+} as follows: 20 mg of IIPs was dispersed in 5 mL of 60 mg L^{-1} Pb^{2+} standard solutions in a 10 mL flask, and then the mixture was continuously oscillated for 20−180 min at room temperature in a thermostatically controlled water bath; the polymers were removed centrifugally. And then the AAS measurement was similar to that of the static adsorption test.

Selectivity experiments were conducted using Cu^{2+}, Cd^{2+}, Zn^{2+}, and Mn^{2+} as comparison ions individually at the same concentration of 20 mg L^{-1} as Pb^{2+}, and interference tests were carried out using Fe^{3+}, Cd^{2+}, Mn^{2+}, Cu^{2+}, Zn^{2+}, Ca^{2+}, and K^+ as concomitant ions, individually at the concentration of 10 times excess (200 mg L^{-1}). The experimental processes were similar to the above static adsorption test with the same polymer mass of 20 mg.

Pb^{2+} Adsorption−Desorption Studies. The reusability of Pb^{2+} IIPs was investigated by the adsorption−desorption studies according to that reported.[25,27] Briefly, the adsorbed Pb^{2+} ions on IIPs could be desorbed by treatment with 0.5 mol L^{-1} HNO_3. In the desorption medium, the Pb-adsorbed IIPs were dispersed, and the mixture solutions were consecutively stirred for 2 h at room temperature. After that, the final concentration of Pb^{2+} released in the solution was determined as described above. By using the identical IIPs to complete 10 cycles of adsorption−desorption, the reusability evaluation of Pb-IIPs was attained.

IIPs-SPE Procedure. The prepared Pb-IIPs (200 mg) were slurred with DDI water and then were poured into a pyrex glass column (4.0 mm i.d.). The column was preconditioned successively with 0.1 mol L^{-1} HNO_3 (5 mL) and DDI water (5 mL). Then the sample solutions (50 mL) containing Pb^{2+} at three concentration levels (5, 20, and 100 μg L^{-1}) were respectively passed through the column at a flow rate of

dx.doi.org/10.1021/am4042405 | ACS Appl. Mater. Interfaces 2014, 6, 305−313

1.0 mL min^{-1}. After that, the column was washed with DDI water (10 mL) and the adsorbed Pb^{2+} was eluted with 0.5 mol L^{-1} HNO_3 (2.5 mL). Finally, the obtained extractants were detected by AAS.

Sample Collection and Preparation. Tap water sample was collected from the laboratory when needed after flowing for about 5 min, and lake water sample was collected from an artificial lake located in Laishan District of Yantai City (China) and was stored at 4 °C in the dark for use. The water samples were collected in Nalgene bottles, and were filtered by 0.45 μm pore size membranes to remove the suspended particles. The resultant filtrates were alkalified to pH 7.0 using 0.1 mol L^{-1} NaOH and were kept in a refrigerator at 4 °C before use. Recoveries were attained by investigating the real water samples spiked with the Pb^{2+} standards at three concentrations (5, 20, and 100 μg L^{-1}), and each concentration was analyzed three replicates, respectively.

RESULTS AND DISCUSSION

Preparation and Characterization of Pb-IIPs. In the Pb-IIPs synthesis process, two types of functional monomers, MAA and 4-VP, were adopted. 4-VP itself possibly forms coordination complexes with lead ions, but its function is more related to its action as a proton acceptor for the MAA; that is, it can assist carboxyl group better dissociation through proton abstraction as a base, which will facilitate the binding of the carboxylate to Pb^{2+} ions, as illustrated in Figure 1b. An ionic complex can be established between the anionic carboxylic acid ligand in MAA and the cationic Pb^{2+} ions via ionic interactions, although the strength of the interaction is actually deficient as the dissociation of the acid goes against water. Therefore, the synergy of 4-VP and MAA plays an important role in the preparation of Pb-IIPs. The solid binding of the template ion to the monomer ligand provides strong imprinting sites. When the Pb-IIPs are used as adsorbents to remove Pb^{2+} ions, the recognition sites and the proper size cavities exactly for Pb^{2+} ions on the surface of the polymers will contribute to a high adsorption efficiency and selectivity for Pb^{2+} ions due to metal–ligand chemistry.[33]

Figure 2 shows the FT-IR spectra of Pb-IIPs and their corresponding NIPs. As seen, the typical peak at 1602 cm^{-1} can be attributed to the stretching vibration of Pb–O, which indicated the formation of Pb-IIPs. However, no peak was observed at the same position for the Pb-removed IIPs and NIPs. The characteristic band of pyridine ring was observed at 1638 cm^{-1}, and the intense peak at 1380 cm^{-1} belonged to the stretching vibration of C–N of 4-VP. Three characteristic peaks of MAA were found at 920, 1261, and 1720 cm^{-1}, which can be assigned to the plane bending vibration of O–H, stretching vibration of C–O and stretching vibration of C═O, respectively. The mutual participation of 4-VP and MAA as functional monomers was evidenced. Also, the broad peak at 1160 cm^{-1} revealed the presence of EGDMA as cross-linker. All the results of FT-IR confirmed that the Pb^{2+} was successfully imprinted based on ionic interaction.

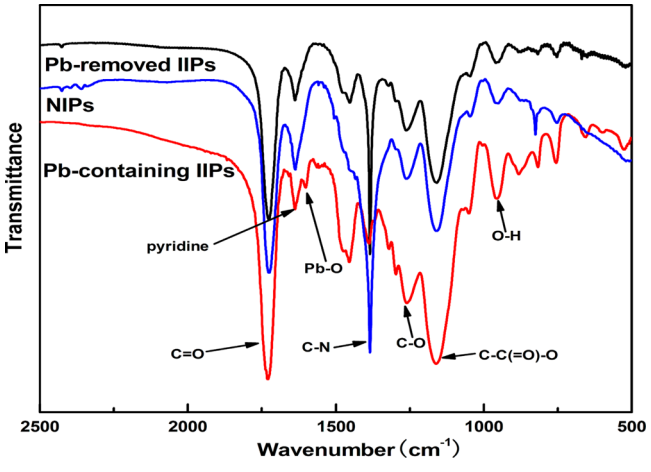

Figure 2. FT-IR spectra of Pb-containing IIPs, Pb-removed IIPs, and corresponding NIPs.

Figure 3 shows the SEM images of the B-IIPs and S-IIPs. As displayed, irregular bulk particles were synthesized by bulk polymerization (Figure 3a), while uniform spherical particles with a diameter of 300–400 nm were synthesized by suspension polymerization (Figure 3b–d). Probably, the adsorption performance of S-IIPs would be better than that of the B-IIPs, owing to their regular morphology and thereby higher surface area than the later. In addition, by BET analysis, the specific surface area of S-IIPs was attained as 1871.6 m^2/g, much higher than that of B-IIPs (36.1 m^2/g), as seen in Table S1 in the Supporting Information. And Figure S1 shows N_2 adsorption–desorption isotherms and pore size distribution of S-IIPs and B-IIPs.

TGA, by referring to a thermal analysis technique, measures the relationship between the weight of sample and the temperature change under controllable temperatures. The temperature range over which a mixture of compounds melts depends on their relative amounts.[34] Figure S2 shows the TGA curves of S-IIPs, B-IIPs, and S-NIPs with similar trends except for the residues. With the increase of temperature from 50 to 100 °C, their weight loss was mainly owing to the evaporation and disappearance of adsorbed water. As the temperature changed from 100 to 300 °C, the weight decreased at a low loss rate, while ranging from 300 to 450 °C a high loss rate was displayed. The peak temperatures of S-IIPs, B-IIPs, and S-NIPs were 424, 416.5, and 434 °C, respectively, and the corresponding residual amounts were 26.16, 7.34, and 19.77%, respectively. The weight loss might well result from the decomposition and degradation of polymers. Consequently, the S-IIPs were fully demonstrated to possess good thermal stability when the temperature was lower than 300 °C.

Binding Studies of the IIPs. The influence of pH on Pb^{2+} adsorption by the polymers is shown in Figure 4. Since metal precipitation might possibly occur as well as IIPs selectivity might well decrease, the pH higher than 7 was not investigated. As seen from the figure, with the increase of pH, adsorption capacity of the two polymers gradually increased. The reason is very likely owing to that the competition from the hydrogen ions decreased and more Pb^{2+} ions could be adsorbed on the polymers with increasing pH value. The maximum adsorption capacity was observed around neutral environment and the S-IIPs presented higher adsorption than B-IIPs. Thus, pH 7.0 was selected for all further work.

Dynamic binding experiments were carried out to evaluate the ionic transfer properties of the IIPs prepared by two different methods. Figure 5a shows that the adsorption amounts of both S-IIPs and B-IIPs for Pb^{2+} ions increased with time increasing. Excitedly, the S-IIPs provided more rapid adsorption for Pb^{2+} than that of the B-IIPs, as well as higher equilibrium binding capacity within 2 h. Moreover, the S-IIPs presented better dynamic binding performances than that of S-IIPs-MAA and S-IIPs-VP, prepared using single functional monomers, as seen in Figure S3a. These results indicated the

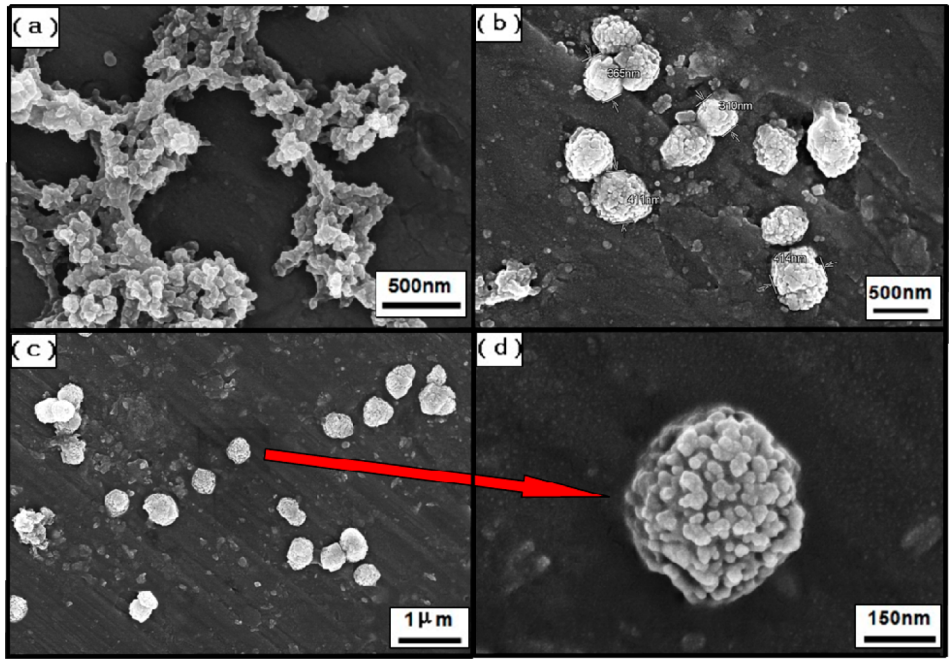

Figure 3. SEM microphotographs of B-IIPs (a) and S-IIPs (b–d).

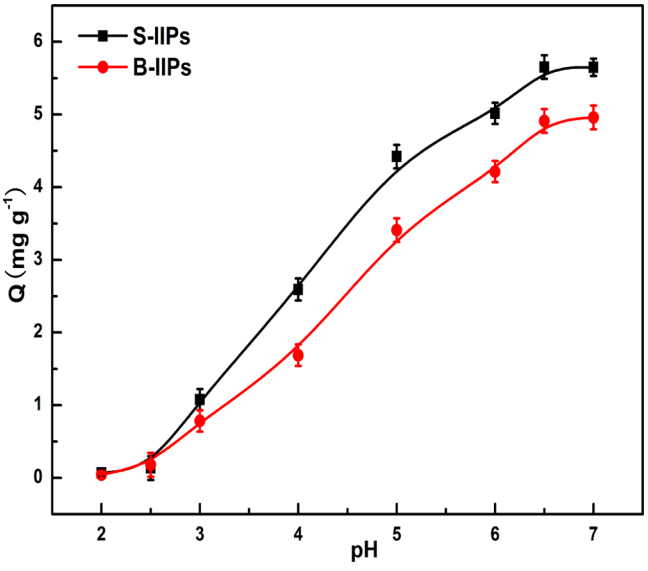

Figure 4. Effect of pH on adsorption capacity of Pb-IIPs. Pb^{2+} initial concentration, 60 mg L^{-1}; adsorption time, 3 h; IIPs, 20 mg; temperature, 25 °C.

uniform spherical structure and larger specific surface area of the S-IIPs were in favor of binding capacity and mass transfer.

The dynamic binding was further investigated by using different models including pseudo-first-order, pseudo-second-order, Elovich and intraparticle diffusion,[35] and the obtained fitting results were summarized in Table 1. With the highest correlation coefficient of R^2 = 0.9504, intraparticle diffusion model offered the most suitable correlation for the adsorption of Pb^{2+} on the S-IIPs. A process is diffusion controlled if its rate depends on the rate at which components diffuse toward each other. The intraparticle diffusion equation can be expressed as

$$Q_t = k_{id} t^{1/2} + C \quad (2)$$

where k_{id} stands for the intraparticle diffusion rate (mg g^{-1} $min^{-1/2}$), C is a constant of the boundary layer thickness. As shown from Figure 5b, the curve in the entire time period is not always linear. It demonstrates that there are several steps affecting the adsorption of Pb^{2+}. At the beginning, it might be owing to the spread of Pb^{2+} from the solution to the outside of IIPs. The second step started with a faster transfer rate to thread the large aperture of IIPs, and then passed through the small aperture at a lower speed. It can be deduced that the internal diffusion of particles was the process of speed limit. The third step is the equilibrium phase which marked reaching steady state. Because IIP imprinting sites tended to be saturated and the low concentration Pb^{2+} ions were left, the intraparticle diffusion presented a weak activity. Therefore, it can be concluded the adsorption followed intraparticle diffusion kinetics model.

Figure 5c shows the binding isotherms of Pb^{2+} onto the S-IIPs, S-NIPs, and B-IIPs. The curves were obtained by plotting the correlation of saturated adsorption amounts of polymers and equilibrium concentrations of Pb^{2+}. As we can see, the adsorption capacity for Pb^{2+} increased quickly with its initial concentration increasing. When the equilibrium concentration was higher than 80 mg L^{-1}, adsorption amounts of S-IIPs became stable and its recognition sites were almost completely occupied by Pb^{2+} ions. S-NIPs and B-IIPs exhibited the same trend as S-IIPs with lower saturated adsorption amounts. As seen, the S-IIPs possessed the higher binding capacity than the B-IIPs and that of the corresponding control S-NIPs. Moreover, the S-IIPs presented better binding characteristics than that of using single functional monomers, as shown in Figure S3b. Therefore, the S-IIPs possessed favorable access and removal ability for template Pb^{2+} ions.

Scatchard analysis was used to further evaluate the binding isotherms. According to the Scatchard equation that was described in reference,[36] the plots for Pb^{2+} adsorbed onto the polymers were obtained. As shown in Figure S4, there were two apparent sections within the plot of S-IIPs that could be regarded as two straight lines. The results meant that there

dx.doi.org/10.1021/am4042405 | ACS Appl. Mater. Interfaces 2014, 6, 305–313

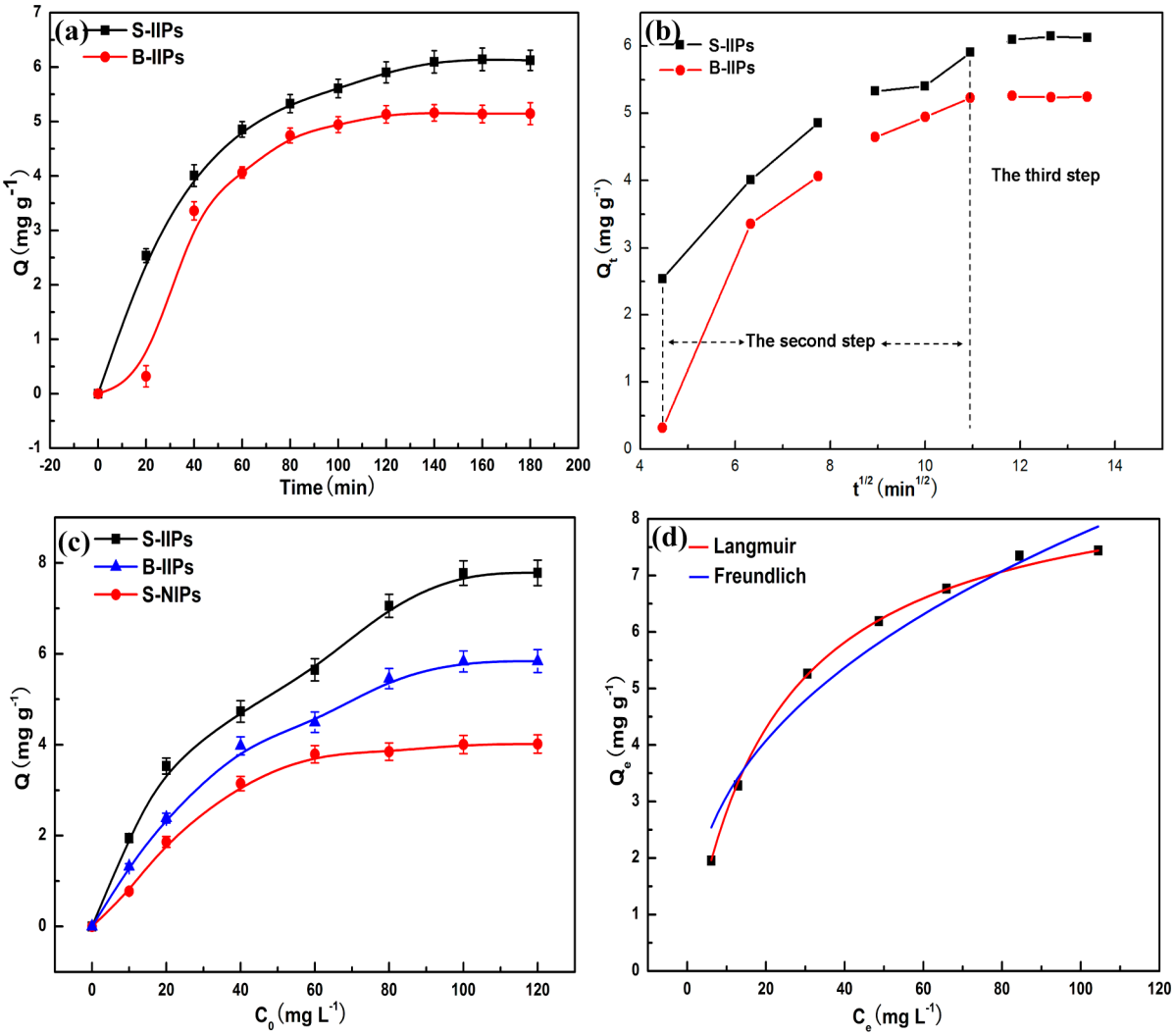

Figure 5. (a) Kinetic uptake of Pb^{2+} onto the S-IIPs and B-IIPs and (b) nonlinear regression of interparticle diffusion kinetic model for S-IIPs. Experimental conditions: V = 10 mL; initial concentration, C_0 = 60 mg L^{-1}; mass of polymer, 20 mg. (c) Binding isotherms of Pb^{2+} onto the S-IIPs, B-IIPs, and S-NIPs in acetonitrile and (d) Langmuir and Freundlich isotherm models for Pb^{2+} adsorption onto S-IIPs. C_e, equilibrium concentration. Experimental conditions: V = 10 mL; mass of polymer, 20 mg; adsorption time, 3 h.

Table 1. Parameters Obtained for Pb^{2+} Adsorption onto the S-IIPs from Different Kinetic Models[a]

model	equation	parameters		R^2
pseudo-first-order	$\log(Q_e - Q_t) = \log Q_e - \frac{k_1}{2.303}t$	k_1 (min^{-1}), 0.0333	Q_e (mg g^{-1}), 9.04	0.9447
pseudo-second-order	$\frac{t}{Q_t} = \frac{1}{k_{ad}Q_e^2} + \frac{t}{Q_e}$	k_{ad} (g mg^{-1} min^{-1}), 0.3012	Q_e (mg g^{-1}), 9.35	0.8763
Elovich	$Q_t = \frac{1}{\beta}\ln(a\beta) + \frac{1}{\beta}\ln(t)$	α (mg g^{-1} min^{-1}), 0.45	β (g mg^{-1}), 4.35	0.7092
intraparticle diffusion	$Q_t = k_{id}t^{1/2} + C$	k_{id} (mg g^{-1} $min^{-0.5}$), 0.3842	C (mg g^{-1}), 1.47	0.9504

[a] Q_t is the solid-phase loading of Pb^{2+} in the adsorbent at time t, Q_e is the adsorption capacity at equilibrium, k_1 is the rate constant of pseudo-first-order adsorption. In the pseudo-second-order model, k_{ad} is the rate constant of adsorption. α and β represent the initial adsorption rate and desorption constant in Elovich model. k_{id} indicates the intraparticle diffusion rate constant, and C provides information about the thickness of the boundary layer.

were two kinds of binding sites for the S-IIPs, and the rebinding sites were primarily related to metal–ligand chemistry.[33] In contrast, the nonlinearity for NIPs suggested there were no selective recognition sites for Pb^{2+} on the polymers (data not shown). From the Scatchard analysis, it could be supposed that the rebinding in the IIPs was largely dependent on metal–ligand interaction, while the interaction between NIPs and Pb^{2+} was mainly from nonspecific adsorption such as van der Waals. Consequently, the Q_{max} (maximum adsorption capacity) was calculated, that is, 8.35 mg/g for S-IIPs, and 3.96 mg/g for NIPs, and thereby the imprinting factor was attained of 2.1, as well as 6.08 mg/g for B-IIPs. These results indicated that the

imprinting process through ionic interaction by using two functional monomers created more imprinting cavities, which led to the higher binding capacity for template ions.

As for the sorption isotherm models, Langmuir, Freundlich and Langmuir−Freundlich isotherm parameters for adsorption of Pb^{2+} onto the S-IIPs and B-IIPs are displayed in Table S2. Their corresponding equations are given in the Supporting Information (eq S1). It can be observed that the Langmuir isotherm model yielded a better fit than that by the Freundlich and Langmuir−Freundlich models, for correlation coefficients (R^2) above 0.99. As can be seen, Figure 5d shows the equilibrium data for Langmuir and Freundlich isotherms, which further confirmed that the Langmuir isotherm model was suitable to the S-IIPs adsorptions for Pb^{2+}.

Selectivity and Anti-Interference Examinations of the S-IIPs. Both selectivity and anti-interference examinations were carried out, since selectivity is a primary concern index to estimate IIPs performances. One kind of experiments were to test adsorption capacity and selectivity coefficient of the IIPs in their respective existence of Cu^{2+}, Cd^{2+}, Zn^{2+}, and Mn^{2+}, at the same concentration as Pb^{2+} (20 mg L^{-1}). The other kind of experiments were to test adsorption capacity of the IIPs toward the mixture solutions containing Pb^{2+} (20 mg L^{-1}) and various possible interference ions with separate presence individual at 10 times (200 mg L^{-1}) excess.

Competitive adsorption for Cu^{2+}, Cd^{2+}, Zn^{2+}, and Mn^{2+}, which are commonly present in water samples, on Pb-IIPs was investigated to evaluate the selective binding of IIPs. As can be seen from Table 2, both the S-IIPs and B-IIPs provided higher

Table 2. Competitive Adsorption Parameters of the Prepared Polymers[a]

	S-IIPs		B-IIPs		S-NIPs	
metal ions	Q	k^b	Q	k	Q	k
Pb^{2+}	2.40		1.91		0.72	
Cu^{2+}	0.080	30.00	0.110	17.36	0.062	11.61
Cd^{2+}	0.063	38.09	0.072	26.53	0.051	14.12
Zn^{2+}	0.056	42.86	0.064	29.84	0.047	15.32
Mn^{2+}	0.075	32.00	0.083	23.01	0.056	12.86

[a]Experiment conditions: mass of polymers, 20 mg; solution initial concentration, C_0 = 20 mg L^{-1}; solution volume, 10 mL; adsorption time, 2 h; room temperature. [b]$k = Q_{template}/Q_{competetive\ ion}$. $Q_{template}$ and $Q_{competetive\ ion}$ are adsorption capacity of the template and competitive ions on IIPs or NIPs, respectively.

adsorption capacities for Pb^{2+} than that for the other four ions. Moreover, the S-IIPs offered higher binding capacities and selectivity coefficients for Pb^{2+} than that of the B-IIPs. For example, the selectivity coefficients of S-IIPs for Pb^{2+}/Cd^{2+} and Pb^{2+}/Zn^{2+} were 38 and 43, respectively, while those of B-IIPs were 27 and 30, respectively, which is very likely owing to the formation of a more stable complex between MAA and Pb^{2+} through ionic interactions with the aid of 4-VP, by suspension polymerization. Therefore, the prepared S-IIPs had an excellent selectivity for Pb^{2+}.

The adsorption capacities for Pb^{2+} on the IIPs in the presence of other possible interference ions, including Fe^{3+}, Cd^{2+}, Mn^{2+}, Cu^{2+}, Zn^{2+}, Ca^{2+}, and K^+, were evaluated for further examination of the anti-interference ability of the Pb-IIPs. As evidenced in Figure 6, those foreign ions did not cause significant interference without remarkable adsorption capacity reduction for Pb^{2+} on S-IIPs, and it could be estimated that

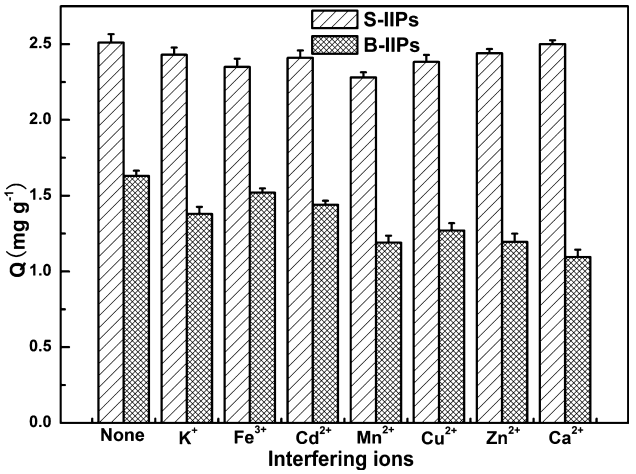

Figure 6. Binding capacity for Pb^{2+} in the presence of 20 mg L^{-1} Pb^{2+} and 200 mg L^{-1} other metal ions, including Fe^{3+}, Cd^{2+}, Mn^{2+}, Cu^{2+}, Zn^{2+}, Ca^{2+}, and K^+.

only <15% of binding sites were taken over by the 10 times foreign ions; in contrast, the adsorption capacity for Pb^{2+} on B-IIPs dramatically declined almost 25−40%. This revealed that the S-IIPs prepared by suspension polymerization, based on ionic interactions by means of the synergy of dual functional monomers, had higher selectivity for Pb^{2+} than the B-IIPs prepared by conventional bulk polymerization. Therefore, the S-IIPs possessed strong anti-interference ability and they could highly selectively, reliably recognize Pb^{2+}.

Reusability of the S-IIPs. Besides the above-mentioned selectivity, reusability is also an important index, since it plays a key role in realizing cost-effectiveness of the IIPs. First, we investigated desorption of the adsorbed Pb^{2+} from the S-IIPs, and obtained over 93% desorption efficiency through 3 h treatment by using 0.5 mol L^{-1} HNO_3 as desorption medium. Then, adsorption−desorption cycle experiments were conducted to display the reusability of the S-IIPs. After repeating 10 times, a good recoverability was attained with the standard error within 5%. Consequently, the prepared novel S-IIPs were demonstrated to be excellently suited for reuse without remarkable decrease in their adsorption capacities for Pb^{2+}.

SPE Condition Optimization Using S-IIPs as Sorbents. Accordingly, the highly selective and reliable S-IIPs were employed as SPE sorbents for preconcentration of Pb^{2+}. To attain optimal extraction recoveries in a short time, related influence factors were investigated, including flow rate of loading sample, loading volume, and the elution conditions such as elution volume, eluent flow rate, and eluent concentration. It is well-known that the flow rate and volume of loading sample solution have very important effects on the adsorption amounts and analytical time. In order to avoid a long analytical time, the flow rates <0.5 mL min^{-1} were not studied. Herein, the effect of flow rate in the range of 0.5−2.0 mL min^{-1} was investigated. Generally speaking, adsorption amounts and recovery values decrease with sample flow rate increasing. Experimental results suggested that at a flow rate of 0.5−1.0 mL min^{-1}, the Pb^{2+} ions could be quantitatively adsorbed by the S-IIPs with the efficiency > 95%. However, at a flow rate over 1.0 mL min^{-1}, quantitation became very difficult and percentage adsorption decreased (<95%), which might be well because Pb^{2+} could not properly equilibrate with the sorbent. Hence, 0.5 mL min^{-1} was finally chosen as an

dx.doi.org/10.1021/am4042405 | ACS Appl. Mater. Interfaces 2014, 6, 305−313

optimum sample rate for a more rapid operation with higher recovery. Meanwhile, different volumes (20, 50, and 80 mL) of sample solutions containing 0.1 mg L^{-1} Pb^{2+} at pH 7.0 were respectively passed through the S-IIPs column in order to determine the loading volume that can be concentrated with the acceptable level of recoveries. When the sample volume was lower than 80 mL, the recovery higher than 95% was attained. So, 0.5 mL min^{-1} and 50 mL were selected as the optimal flow rate and loading volume of sample solution, respectively, in the following work, in view of the higher recovery and shorter analytical time. On the other hand, elution conditions such as elution volume, eluent flow rate, and eluent concentration are widely recognized as important parameters to affect the SPE recoveries. So, different eluent volumes between 2 and 8 mL, different flow rates varying from 0.5 to 2 mL min^{-1}, and different eluent concentrations in a range of 0.25−1 mol/L HNO_3 were investigated in order to find optimum elution conditions. Finally, 2.5 mL of 0.5 mol L^{-1} HNO_3 at 0.5 mL min^{-1} was adopted for elution.

Analytical Performances and Applications of the S-IIPs-SPE to Water Samples. Under the above optimized conditions, the analytical performances based on S-IIPs-SPE were investigated. An excellent linearity over the concentration range from 0.2 to 50 μg L^{-1} was presented, with the equation of $y = 0.02724x + 0.00016$, ($R^2 = 0.9998$), where y and x are absorbance and concentration of Pb^{2+} in μg L^{-1}, respectively, as shown in Figure S5. The limit of detection (LOD) based on 3SD/m and the limit of quantification (LOQ) based on 10SD/m,[31] where SD is the standard deviation of 9 consecutive measurements of the blank and m is the mean slope of the calibration curve, were attained of 0.06 and 0.19 μg L^{-1}, respectively, for Pb^{2+}. The repeatability of the S-IIPs-SPE was assessed by analyzing the same standard solutions 5 times. The relative standard deviation (RSD) for the determination of 10 μg L^{-1} Pb^{2+} was achieved of 2.8%.

Furthermore, the S-IIPs-SPE was applied for the preconcentration of trace Pb^{2+} in tap and lake water samples to evaluate the practicality of the developed method. The recovery experiments were performed using a standard addition method by spiking the Pb^{2+} solutions at three concentration levels (5, 20, and 100 μg L^{-1}) and analyzing three replicates for each concentration. As listed in Table 3, the recovery values varying from 95.5 to 104.6% were obtained, with the RSD in the range of 2.2−4.3%, which indicated the obtained S-IIPs based on ionic interaction by utilizing the synergy of two functional monomers were ideal candidates for SPE sorbents, and were potentially applicable to effectively preconcentrate and quantitatively determine trace Pb^{2+} in real water samples. Meanwhile, the results suggested matrix effects could be significantly reduced by utilizing the S-IIPs-SPE procedure. Furthermore, it should be noted that the endogenous content of Pb^{2+} was detected at 0.16 μg L^{-1} in the tested lake water sample. The value is much lower than the maximum contaminant level for Pb^{2+} in drinking water, namel,y 14.9 μg L^{-1} (72 nM) regulated by the United States Environmental Protection Agency. Therefore, the validated method of S-IIPs-SPE pretreatment procedure coupled to AAS detection technology holds great potentials as an ideal alternative to simultaneous separation, enrichment, and determination of Pb^{2+} in real water samples for pollution monitoring and abatement.

Table 3. S-IIPs-SPE Recoveries (%) and Relative Standard Deviations (RSD, %) Obtained from Analysis of Water Samples Spiked with Pb^{2+}[a]

sample	added (μg L^{-1})	found (μg L^{-1})	recovery ± RSD[bc]
tap water	0	0	
	5	4.96	97.5 ± 2.2
	20	20.08	100.4 ± 3.1
	100	99.97	96.7 ± 2.7
lake water	0	0.16	
	5	4.86	95.5 ± 3.5
	20	19.57	96.3 ± 2.8
	100	100.32	104.6 ± 4.3

[a]Experimental conditions: loading volume, 50 mL; loading rate, 0.5 mL min^{-1}; washing, 10 mL of DDI water; eluting, 2.5 mL of 0.5 mol L^{-1} HNO_3. [b]Average value from three individual experiments. [c]$n = 3$.

Method Performance Comparisons. Method performance of this developed dual functional monomer imprinting strategy toward Pb^{2+} was compared with that of some reported IIPs based methods, as listed in Table S3. As shown from the table, single functional monomers of 4-VP, 2-VP, DEM (2-(diethylamino) ethyl methacrylate), and chitosan, commercially available and commonly used monomers in the synthesis of MIPs/IIPs, are utilized,[29,32,31,28] and the coaction of 4-VP and self-synthesized DDDPA (1,12-dodecanediol-*O*,*O*′-diphenylphosphonic acid) is also employed,[30] for Pb^{2+} imprinting. Our work demonstrates higher sensitivity and wider linear range than that reported using precipitation polymerization[29,31] or bulk polymerization,[32] all with SPE procedures followed by AAS[29,32] or ICP-OES[31] detection. Also, herein, higher selectivity coefficients are obtained than that using surface imprinting on mesoporous silica SBA-15,[31] or the coefficients are comparable to that using DEM as functional monomer.[28] The W/O/W emulsion polymerization along with two functional monomers shows a higher selectivity coefficient for Pb^{2+} related to Cd^{2+} and a wider pH range;[30] however, we not only utilize easily obtained commercial monomer avoiding complex synthesis/characterization, but also systematically investigate analytical performance and further applications to practical water samples. On the other hand, compared with the previous work by Hoai et al. using the same dual functional monomers,[15] we have carried out more comprehensive and profound studies for Pb^{2+} and thereby will further develop dual/multiple functional monomer based imprinting strategies. Therefore, overall, the superiority of our obtained Pb^{2+} IIPs and related methods are very obvious on account of the excellent selectivity, reliability, and sensitivity. Moreover, they are simple and easy to prepare and use as well as have the promising application potentials in enrichment and/or removal of Pb^{2+} from polluted water samples.

CONCLUSIONS

In conclusion, the new Pb-IIPs were successfully prepared based on ionic interaction via synergy of dual functional monomers and were applied as SPE sorbents to highly selective cleanup and preconcentration of trace Pb^{2+} in water samples. Two common functional monomers which could provide an excellent synergy effect were utilized for suspension polymerization, and the resultant IIPs displayed fast adsorption kinetics and high binding capacity for Pb^{2+}. The adsorption behavior of Pb^{2+} onto IIPs followed intraparticle diffusion kinetics model. Langmuir model was well fitted with the static adsorption data,

and this indicated the monolayer coverage of Pb^{2+} ions was formed at the surface of the IIPs sorbent. Competitive adsorption studies showed that the IIPs by suspension polymerization offered a number of excellent advantages such as high selectivity and reliability toward targeted Pb^{2+} ions compared with that by bulk polymerization, even in the presence of other metal ions.

On the other hand, by virtue of the Pb^{2+} imprinting, an analytical model of proof-of-concept, we intend to develop a general applicable recognition and detection platform. With the appropriate choice and reasonable utilization of ionic interaction and dual/multiple functional monomers and, furthermore, by smartly devising and synthesizing new functional monomers, the IIPs-based heavy metal ion detection platform can be constructed and developed for selective and sensitive routing monitoring of water quality. Besides improving the selectivity of IIPs/MIPs, utilization of dual/multiple functional monomers commercially available and delicate design and synthesis of new functional monomers are effective ways to imprint various analytes and therefore to push forward the development of molecular imprinting techniques.

■ ASSOCIATED CONTENT

Supporting Information

BET analysis results and TGA curves of S-IIPs, B-IIPs, and S-NIPs. Kinetic and static adsorption curves of S-IIPs using single functional monomers, as well as analytical curve for Pb^{2+} with S-IIPs-SPE procedure. Langmuir, Freundlich, and Langmuir–Freundlich isotherms fitting parameters, as well as method performance comparisons for Pb^{2+} with other IIPs based methods. This material is available free of charge via the Internet at http://pubs.acs.org.

■ AUTHOR INFORMATION

Corresponding Authors

*E-mail: jhli@yic.ac.cn (J.L.).

*E-mail: lxchen@yic.ac.cn (L.C.). Tel/Fax: +86 535 2109133, +86 535 2109130.

Notes

The authors declare no competing financial interest.

■ ACKNOWLEDGMENTS

This work was financially supported by the National Natural Science Foundation of China (21275158, 21105117), the Scientific Research Foundation for the Returned Overseas Chinese Scholars, State Education Ministry, and the 100 Talents Program of the Chinese Academy of Sciences.

■ REFERENCES

(1) Naser, H. A. *Mar. Pollut. Bull.* **2013**, *72*, 6–13.
(2) Fu, F. L.; Wang, Q. *J. Environ. Manage.* **2011**, *92*, 407–418.
(3) Nzihou, A.; Stanmore, B. *J. Hazard. Mater.* **2013**, *256–257*, 56–66.
(4) Pala, I. R.; Brock, S. L. *ACS Appl. Mater. Interfaces* **2012**, *4*, 2160–2167.
(5) Sohrabi, M. R.; Matbouie, Z.; Asgharinezhad, A. A.; Dehghani, A. *Microchim. Acta* **2013**, *180*, 589–597.
(6) Liu, C. K.; Bai, R. B.; Ly, Q. S. *Water Res.* **2008**, *42*, 1511–1522.
(7) Martins, B. L.; Cruz, C. C. V.; Luna, A. S.; Henriques, C. A. *Biochem. Eng. J.* **2006**, *27*, 310–314.
(8) Li, C. X.; Gao, J.; Pa, J. M.; Zhang, Z. L.; Yan, Y. S. *J. Environ. Sci.* **2009**, *21*, 1722–1729.
(9) Pan, D. W.; Wang, Y.; Chen, Z. P.; Lou, T. T.; Qin, W. *Anal. Chem.* **2009**, *81*, 5088–5094.
(10) Fu, X. L.; Lou, T. T.; Chen, Z. P.; Lin, M.; Feng, W. W.; Chen, L. X. *ACS Appl. Mater. Interfaces* **2012**, *4*, 1080–1086.
(11) Rehman, R.; Anwar, J.; Mahmud, T. *Desalin. Water Treat.* **2013**, *51*, 2624–2634.
(12) Aragay, G.; Pons, J.; Merkoci, A. *Chem. Rev.* **2011**, *111*, 3433–3458.
(13) Timerbaev, A. R. *Chem. Rev.* **2013**, *113*, 778–812.
(14) Pan, J. Y.; Wang, S.; Zhang, R. F. *Anal. Chem.* **2006**, *86*, 855–865.
(15) Hoai, N. T.; Yoo, D. K.; Kim, D. *J. Hazard. Mater.* **2010**, *173*, 462–467.
(16) Madadrang, C. J.; Kim, H. Y.; Gao, G. H.; Wang, N.; Zhu, J.; Feng, H. *ACS Appl. Mater. Interfaces* **2012**, *4*, 1186–1193.
(17) Song, X. L.; Li, J. H.; Xu, S. F.; Ying, R. J.; Ma, J. P.; Liao, C. Y.; Liu, D. Y.; Yu, J. B.; Chen, L. X. *Talanta* **2012**, *99*, 75–82.
(18) Chen, L. X.; Xu, S. F.; Li, J. H. *Chem. Soc. Rev.* **2011**, *40*, 2922–2942.
(19) Shen, X. T.; Zhu, L. H.; Wang, N.; Ye, L.; Tang, H. Q. *Chem. Commun.* **2012**, *48*, 788–798.
(20) Li, J. H.; Zhang, Z.; Xu, S. F.; Chen, L. X.; Zhou, N.; Xiong, H.; Peng, H. L. *J. Mater. Chem.* **2011**, *21*, 19267–19274.
(21) Xu, S. F.; Lu, H. Z.; Li, J. H.; Song, X. L.; Wang, A. X.; Chen, L. X.; Han, S. B. *ACS Appl. Mater. Interfaces* **2013**, *5*, 8146–8154.
(22) Li, J. H.; Wen, Y. Y.; Chen, L. X. *Chin. J. Chromatogr.* **2013**, *31*, 181–184.
(23) Batlokwa, B. S.; Chimuka, L.; Tshentu, Z.; Cukrowska, E.; Torto, N. *Water SA.* **2012**, *38*, 255–260.
(24) Li, C. X.; Gao, J.; Pan, J. M.; Zhang, Z. L.; Yan, Y. S. *J. Environ. Sci.* **2009**, *21*, 1722–1729.
(25) Pakade, V. E.; Cukrowska, E. M.; Darkwa, J.; Darko, G.; Torto, N.; Chimuka, L. *Water Sci. Technol.* **2012**, *65*, 728–736.
(26) Preetha, C. R.; Gladis, J. M.; Rao, T. P. *Environ. Sci. Technol.* **2006**, *40*, 3070–3074.
(27) Xu, S. F.; Chen, L. X.; Li, J. H.; Guan, Y. F.; Lu, H. Z. *J. Hazard. Mater.* **2012**, *237–238*, 347–354.
(28) Liu, Y.; Liu, Z. C.; Gao, J.; Dai, J. D.; Han, J.; Wang, Y.; Xie, J. M.; Yan, Y. S. *J. Hazard. Mater.* **2011**, *186*, 197–205.
(29) Mostafa, K.; Heidari, Z. S.; Sanchooli, E. *Chem. Eng. J.* **2011**, *166*, 1158–1163.
(30) Zhu, L. Y.; Zhu, Z. L.; Zhang, R. H.; Hong, J.; Qiu, Y. L. *J. Environ. Sci.* **2011**, *23*, 1955–1961.
(31) García-Otero, N.; Teijeiro-Valiño, C.; Otero-Romaní, J.; Peña-Vázquez, E.; Moreda-Piñeiro, A.; Bermejo-Barrera, P. *Anal. Bioanal. Chem.* **2009**, *395*, 1107–1115.
(32) Behbahani, M.; Bagheri, A.; Taghizadeh, M.; Salarian, M.; Sadeghi, O.; Adlnasab, L.; Jalali, K. *Food Chem.* **2013**, *138*, 2050–2056.
(33) Becker, J. J.; Gagnea, M. R. *Acc. Chem. Res.* **2004**, *37*, 798–804.
(34) Zhang, Z.; Xu, S. F.; Li, J. H.; Xiong, H.; Peng, H. L.; Chen, L. X. *J. Agric. Food Chem.* **2012**, *60*, 180–187.
(35) Zhu, J. H.; Wei, S. Y.; Gu, H. B.; Rapole, S. B.; Wang, Q.; Luo, Z. P.; Haldolaarachchige, N.; Young, D. P.; Guo, Z. H. *Environ. Sci. Technol.* **2012**, *46*, 977–985.
(36) Xu, S. F.; Li, J. H.; Chen, L. X. *J. Mater. Chem.* **2011**, *21*, 4346–4351.